Band geometry of fractional topological insulators

Rahul Roy

Department of Physics and Astronomy, University of California, Los Angeles, California 90095, USA

(Received 15 August 2012; revised manuscript received 12 August 2014; published 30 October 2014)

Recent numerical simulations of flat-band models with interactions which show clear evidence of fractionalized topological phases in the absence of a net magnetic field have generated a great deal of interest. We provide an explanation for these observations by showing that the physics of these systems is the same as that of conventional fractional quantum Hall phases in the lowest Landau level under certain ideal conditions which can be specified in terms of the Berry curvature and the Fubini-Study or quantum metric of the topological band. In particular, we show that when these ideal conditions hold, the density operators projected to the topological band obey the W_∞ algebra. Our approach leads us to propose a way of testing the suitability of topological bands for hosting fractionalized phases.

DOI: 10.1103/PhysRevB.90.165139 PACS number(s): 73.43.−f, 03.65.Vf, 71.70.Di

I. INTRODUCTION

The advent of topological insulators, which are band insulators with topologically nontrivial bands, has generated a great deal of recent interest in topological phases [1–3]. The Landau levels whose filling gives rise to the integer quantum Hall effect [4] can also be regarded as topologically nontrivial bands. While the integer quantum Hall effect has so far only been observed in the presence of large magnetic fields, a quantized Hall conductance can also arise in the presence of a periodic potential, where it can be related to the Chern invariant, a topological invariant, associated with the bands of Bloch wave functions [5]. Occupied bands of an insulator which have a nontrivial Chern invariant are called Chern bands. In the absence of any time-reversal symmetry breaking, the Chern invariant has to be zero. However, there exist tight-binding models which explicitly demonstrate that a quantized Hall conductance is possible in a zero net external magnetic field, albeit which break time-reversal symmetry [6].

In the presence of interactions, electrons in fractionally filled Landau levels can form a liquidlike phase with a quantized Hall conductance and a gap to all bulk excitations [7]. This is a topological phase with a nontrivial ground-state degeneracy on a torus and excitations with fractional charge and, depending on the filling fraction, fractional or possibly even non-Abelian statistics. The question of whether similar phases can arise in a band-insulator model has recently been addressed in a series of numerical works by many groups [8–12], which provides clear evidence for the existence of gapped phases possessing many of the signatures of the proposed ground states for fractional quantum Hall states.

We elucidate these surprising developments based on the approach of studying the algebra of projected density operators [13]. We show that under certain ideal conditions which will be specified in detail below, the projected density operators obey a closed algebra which has the same form as the W_∞ algebra of the density operators projected to the lowest Landau level (LLL) [14–17]. The method of generating the low-lying magnetophonon spectrum in the fractional quantum Hall effect (FQHE) based on the single-mode approximation relies crucially on the closure of this algebra. The present work highlights the facts that the topological stability of the Chern number invariant of the single-particle states is not sufficient to guarantee the existence of fractionalized states and that details of the geometry of the single-particle Hilbert space encoded in the distributions of the quantum metric and the Berry curvature play a crucial role in the stability of the fractionalized phases.

The single-particle states of Chern bands are very different from Landau-level wave functions, so it is not *a priori* clear why partially filled Chern bands can display an analog of the FQHE. One set of explanations for these numerical results has been based on trial wave functions constructed either by mapping lowest-Landau-level wave functions in the Landau gauge to Wannier functions [18] or by partonization [19,20]. The spectacular success of model wave functions such as Laughlin's wave function in the theory of the FQHE [21] makes such an approach very attractive. However, the crucial feature of the Laughlin wave function is that it keeps particles apart, and an analytic translation of these model wave functions to an arbitrary Chern band does not necessarily share that property. This, among other reasons, has motivated the search for other explanations.

The essential requirements for the formation of fractional Chern insulators were assumed, in the early numerical work, to be some of the characteristic energetic features of the FQHE. These features are (1) a nearly flat band with a nontrivial topological invariant and (2) short-range interactions whose energy scale is much larger than the width of the nontrivial band but much smaller than the band gap. Under these circumstances, it is reasonable to project the interactions to the topological band, as is usually carried out in the theory of the FQHE. The assumption is that the low-energy spectrum consists of states whose admixture with components from the other bands can be neglected. Even with this assumption, however, there are a number of parameters in the fractional Chern insulator problem which have no counterpart in FQHE physics. First, there is the freedom in choosing the lattice itself, which breaks both continuous translational and rotational symmetries but may have certain discrete point- and space-group symmetries. One may also vary the parameters that determine the detailed form of the interaction, and finally, one can also change the various tight-binding parameters of the single-particle Hamiltonian.

In numerical experiments to date, only a limited portion of this large phase space of possible fractional Chern insulators has been explored. Already, it is clear that there is a great

variation in the stability of fractional Chern insulator states even when the basic energetic criteria listed in the previous paragraph are met. One of the aims of this paper is to identify other criteria which affect the stability of fractional Chern insulator states. Our approach is based on studying the commutation relations of projected density operators, a direction which has yielded some success in analyzing fractional Chern insulators [13,22–24].

II. FLAT-BAND TOPOLOGICAL INSULATORS

Before delving into the role of interactions, we describe the basic framework of (nearly) flat-band topological insulators. Our starting point is a tight-binding model which has topologically nontrivial bands, a famous example of which is the Haldane model on a honeycomb lattice [6]. By varying the tight-binding parameters, one can flatten the energy bands without altering the topology of the band structure [25,26]. The Hamiltonian of an N-band insulator can be written as $\sum_{\mathbf{k},p,q} |\mathbf{k},p\rangle [h(\mathbf{k})]_{pq} \langle \mathbf{k},q|$, where the sum over crystal momenta is restricted to the first Brillouin zone (BZ). (Here and for the remainder of the paper, we will adopt the convention that repeated indices are *not* implicitly summed over.)

The states $|\mathbf{k},p\rangle$ are the Fourier transforms of the localized tight-binding orbital states:

$$|\mathbf{k},p\rangle = \frac{1}{\sqrt{N}} \sum_{\boldsymbol{R}_n} e^{i\mathbf{k}\cdot(\boldsymbol{e}_p+\boldsymbol{R}_n)} |\boldsymbol{R}_n,p\rangle, \tag{1}$$

where $\boldsymbol{e}_p + \boldsymbol{R}_n$ denotes the position of the (localized) pth orbital, $|\boldsymbol{R}_n,p\rangle$, in the nth unit cell situated at the lattice vector $\boldsymbol{R}_n$, and N is the number of unit cells in the system. The matrix $h(\mathbf{k})$ can be diagonalized through an appropriate unitary transformation and the Hamiltonian written in the form $H_K = \sum_{\gamma,\mathbf{k}} E_\gamma(\mathbf{k}) |\mathbf{k},\gamma\rangle\langle\mathbf{k},\gamma|$, where $|\mathbf{k},\gamma\rangle = \sum_p u_p^\gamma(\mathbf{k}) |\mathbf{k},p\rangle$ and $u_j^\gamma(\mathbf{k})$ is a normalized eigenstate of $h(\mathbf{k})$ with eigenvalue $E_\gamma(\mathbf{k})$.

We will use the label α for the topological band of interest. The Berry curvature $B_\alpha(\mathbf{k})$ of the band is defined as

$$B_\alpha(\mathbf{k}) = -i \sum_p \left(\frac{\partial u_p^{\alpha *}}{\partial k_x} \frac{\partial u_p^\alpha}{\partial k_y} - \frac{\partial u_p^{\alpha *}}{\partial k_y} \frac{\partial u_p^\alpha}{\partial k_x} \right), \tag{2}$$

and its integral over the Brillouin zone is

$$\int_{BZ} dk_x\, dk_y\; B_\alpha(\mathbf{k}) = 2\pi C_\alpha, \tag{3}$$

where C_α is the Chern number of the band α. For a topological (Chern) band, C_α is nonzero, and without loss of generality we can take C_α to be a positive integer.

We now consider the role of interactions by adding a term U_{int} to the Hamiltonian. The interactions we consider are generally density-density interactions of the form $U_{\text{int}} = \sum_{i,j} u(|\mathbf{r}_i - \mathbf{r}_j|)$. In the limit of a large band gap, one can safely neglect the mixing between the Chern band and the unfilled bands. If the bandwidth is small compared to the scale of the interactions, $E_\alpha(\mathbf{k})$ may be treated as constant and may be set to zero. With this approximation, the low-energy effective Hamiltonian including interactions has the form $H_{\text{eff}} = \bar{U}_{\text{int}}$, where $\bar{U}_{\text{int}}$ is the interaction projected to the Chern band.

One encounters a similar Hamiltonian in the treatment of interactions in the lowest Landau level in the limit of a large magnetic field. In that case, the effective Hamiltonian of a clean system obtained by projecting density-density interactions to the lowest Landau level has the form

$$H_{\text{LLL}} = \frac{1}{2} \int \frac{d^2\mathbf{q}}{(2\pi)^2} v(\mathbf{q}) \sum_{i\neq j} \overline{\rho}^j_{-\mathbf{q}} \overline{\rho}^i_{\mathbf{q}}, \tag{4}$$

where $\overline{\rho}^i_{\mathbf{q}}$ is the projection of the density operator of the ith particle $e^{-i\mathbf{q}\cdot\mathbf{r}_i}$, to the lowest Landau level.

III. ALGEBRA OF PROJECTED DENSITY OPERATORS

In the LLL problem, the projected density operators $\overline{\rho}_{\mathbf{q}}$ obey the W_∞ algebra, first identified by Girvin, MacDonald, and Platzman [14–17]:

$$[\overline{\rho}_{\mathbf{q}_1}, \overline{\rho}_{\mathbf{q}_2}] = 2i \exp\left(\frac{\mathbf{q}_1 \cdot \mathbf{q}_2 \ell_B^2}{2}\right) \sin\left(\frac{\mathbf{q}_1 \wedge \mathbf{q}_2 \ell_B^2}{2}\right) \overline{\rho}_{\mathbf{q}_1+\mathbf{q}_2}, \tag{5}$$

where $\mathbf{q}_1 \wedge \mathbf{q}_2 \equiv \hat{\mathbf{z}} \cdot (\mathbf{q}_1 \times \mathbf{q}_2)$. This algebra is the quantum version of the algebra of area-preserving diffeomorphisms on the plane and can also be interpreted as that of magnetic translations in a uniform field [27]. Together, the density algebra of Eq. (5) and the effective Hamiltonian of Eq. (4) capture the nontrivial dynamics that arise from projection to the lowest Landau level.

The W_∞ algebra is obeyed by both the single-body density operators $\overline{\rho}^i_{\mathbf{q}}$ and the many-body density operator $\sum_i \overline{\rho}^i_{\mathbf{q}}$. In what follows, we will work exclusively with the single-particle density operator, but the considerations also apply to the many-body density operators.

In the single-mode approximation, the projected density operators generate the spectrum of the low-energy excitations that are relevant for the stability of the FQHE states [14,15]. Suppose the projected density operators of the fractional Chern insulators obey the same algebra as in the LLL and the form of the interactions $v(\mathbf{q})$ are chosen to be similar for the two problems. Then one could reasonably expect the same low-energy physics to ensue [28].

Let us therefore examine the projected density operators of the Chern band, following a strategy outlined in Ref. [13]. Let $P_\alpha = \sum_{\mathbf{k}} |\mathbf{k},\alpha\rangle\langle\mathbf{k},\alpha|$ be the operator that projects to the Chern band. A Taylor expansion of the projected density operator $\bar{\rho}_{\mathbf{q}} = P_\alpha \rho_{\mathbf{q}} P_\alpha$ keeping only terms of order q^2 yields

$$\bar{\rho}_{\mathbf{q}} = P_\alpha - i P_\alpha \mathbf{q}\cdot\mathbf{r} P_\alpha - \tfrac{1}{2} P_\alpha (\mathbf{q}\cdot\mathbf{r})^2 P_\alpha. \tag{6}$$

From this expression, it follows that, provided the Berry curvature $B_\alpha(\mathbf{k})$ is uniform in momentum space (i.e., provided the fluctuations in the Berry curvature can be neglected), up to order q^2 the following relation holds:

$$[\bar{\rho}_{\mathbf{q}_1}, \bar{\rho}_{\mathbf{q}_2}] = i(\mathbf{q}_1 \wedge \mathbf{q}_2) \bar{B}_\alpha P_\alpha, \tag{7}$$

where $\bar{B}_\alpha = 2\pi C_\alpha / A_{BZ}$ is the average Berry curvature and A_{BZ} is the area of the Brillouin zone. One may then assert [13] that this has the same form as the W_∞ algebra of the LLL projected density operators, with $\sqrt{\bar{B}_\alpha}$ playing the role of the magnetic length ℓ_B.

Most band structures do not have a uniform Berry curvature, and thus the relation holds only approximately, even to order q^2. One can, however, make a virtue of what seems like a failing by arguing that the degree of deviation from a uniform Berry curvature provides a way to quantify how good a host a particular band structure is for hosting FQHE-like phases, an expectation that has been confirmed by numerics [29].

It is natural to consider higher-order terms in q in $[\bar{\rho}_{\mathbf{q}_1}, \bar{\rho}_{\mathbf{q}_2}]$. Keeping terms of order q^3 (we consider higher-order terms later on), we find that

$$\begin{aligned}[\bar{\rho}_{\mathbf{q}_1}, \bar{\rho}_{\mathbf{q}_2}] &= i\bar{B}_\alpha(\mathbf{q}_1 \wedge \mathbf{q}_2)[P_\alpha - iP_\alpha(\mathbf{q}_1+\mathbf{q}_2)\cdot \mathbf{r} P_\alpha] \\ &\quad - \frac{i}{2}\sum_{a,b,c}\Big(\frac{q_{1a}q_{2b}q_{2c}}{2}[P_\alpha r_a P_\alpha, P_\alpha(r_b Q_\alpha r_c + r_c Q_\alpha r_b)P_\alpha] \\ &\quad + \frac{q_{1a}q_{1b}q_{2c}}{2}[P_\alpha(r_a Q_\alpha r_b + r_b Q_\alpha r_a)P_\alpha, P_\alpha r_c P_\alpha]\Big), \quad (8)\end{aligned}$$

where $Q_\alpha = I - P_\alpha$ and I is the identity operator. The commutators $[P_\alpha r_a P_\alpha, P_\alpha(r_b Q_\alpha r_c + r_c Q_\alpha r_b)P_\alpha]$ and $[P_\alpha(r_a Q_\alpha r_b + r_b Q_\alpha r_a)P_\alpha, P_\alpha r_c P_\alpha]$ vanish if and only if the Fubini-Study (FS) metric tensor $g^\alpha(\mathbf{k})$ is a constant in the Brillouin zone. The Fubini-Study metric, which here acts as a metric in the space of reciprocal vectors, is a rank-two symmetric tensor with components [30–33]

$$g^\alpha_{ab}(\mathbf{k}) = \frac{1}{2}\sum_p\Bigg[\Big(\frac{\partial u^{\alpha *}_p}{\partial k_a}\frac{\partial u^\alpha_p}{\partial k_b} + \frac{\partial u^{\alpha *}_p}{\partial k_b}\frac{\partial u^\alpha_p}{\partial k_a}\Big) - \sum_q\Big(\frac{\partial u^{\alpha *}_p}{\partial k_b}u^\alpha_p u^{\alpha *}_q\frac{\partial u^\alpha_q}{\partial k_a} + \frac{\partial u^{\alpha *}_p}{\partial k_a}u^\alpha_p u^{\alpha *}_q\frac{\partial u^\alpha_q}{\partial k_b}\Big)\Bigg]. \quad (9)$$

If the metric tensor is constant in the Brillouin zone, then to order q^3, the Chern band projected densities satisfy the W_∞ algebra of projected LLL densities. This leads us to identify the uniformity of the metric tensor in momentum space as an additional criterion for identifying "good" band structures from the point of view of hosting interacting topological phases. Of course, other conditions such as a suitable short-ranged interaction and a proper hierarchy of energy scales are no less important.

We will see that when the band structure satisfies one additional constraint, the Chern band projected densities satisfy the W_∞ algebra of projected LLL densities to *all* orders in q. If one could completely ignore the Fubini-Study metric tensor, i.e., set it to zero, then with the assumption of a constant Berry curvature, the algebra of projected density operators would simply be the Heisenberg algebra and would close at all wavelengths. However, the FS metric *cannot* vanish, as the nontrivial topology of the band structure of a Chern band places constraints on the form of the FS metric tensor. The trace of the FS metric tensor at a given point in k space can be expressed as

$$\begin{aligned}\mathrm{tr}[g^\alpha(\mathbf{k})] &= \langle \mathbf{k},\alpha|(x+iy)(I-P_\alpha)(x-iy)|\mathbf{k},\alpha\rangle \\ &\quad + i\langle \mathbf{k},\alpha|[x(I-P_\alpha)y - y(I-P_\alpha)x]|\mathbf{k},\alpha\rangle. \quad (10)\end{aligned}$$

The positive definiteness of the operators $A^\dagger A$ and $C^\dagger C$, where $A = (I-P_\alpha)(x+iy)P_\alpha$ and $C = (I-P_\alpha)(x-iy)P_\alpha$, implies that

$$\langle \mathbf{k},\alpha|AA^\dagger|\mathbf{k},\alpha\rangle \geqslant 0, \quad \langle \mathbf{k},\alpha|CC^\dagger|\mathbf{k},\alpha\rangle \geqslant 0. \quad (11)$$

From these inequalities and Eq. (10), it follows that

$$\mathrm{tr}[g^\alpha(\mathbf{k})] \geqslant |B_\alpha(\mathbf{k})|. \quad (12)$$

Thus the magnitude of the Berry curvature places a lower bound on the trace of the Fubini-Study metric.

One may define transformed operators $r'_a = \sum_b t_{ab} r_b$ corresponding to rotations and scale transformations. Here t is an invertible matrix and $r_1 = x$, $r_2 = y$.

We may also define a corresponding transformed FS metric $g^{\alpha'}(\mathbf{k})$:

$$g^{\alpha'}_{ab}(\mathbf{k}) = \tfrac{1}{2}\langle \mathbf{k},\alpha|[r'_a(I-P_\alpha)r'_b + r'_b(I-P_\alpha)r'_a]|\mathbf{k},\alpha\rangle. \quad (13)$$

Thus $g^{\alpha'}_{ab}(\mathbf{k}) = t_{ac}g^\alpha_{cd}(\mathbf{k})t_{bd}$. Similarly, the transformed Berry curvature is

$$B'_\alpha(\mathbf{k}) = \sum_{a,b}\epsilon_{ab}\langle \mathbf{k},\alpha|r'_a P_\alpha r'_b|\mathbf{k}',\alpha\rangle. \quad (14)$$

If one chooses t such that it corresponds to a unimodular coordinate transformation with $\det[t] = 1$, the Berry curvature is left unchanged, i.e., $B'_\alpha(\mathbf{k}) = B_\alpha(\mathbf{k})$. Inequality (12) then also applies to the transformed FS metric and Berry curvature. Thus

$$\mathrm{tr}[g^{\alpha'}(\mathbf{k})] \geqslant |B_\alpha(\mathbf{k})|. \quad (15)$$

One can always find a unimodular transformation such that the transformed metric at any given point $\mathbf{k}_0$ is a diagonal matrix. Since the determinant of the FS metric is preserved through such a transformation, the transformed metric may be written as

$$g^{\alpha'}(\mathbf{k}_0) = \begin{pmatrix}\sqrt{\det[g^\alpha(\mathbf{k}_0)]} & 0 \\ 0 & \sqrt{\det[g^\alpha(\mathbf{k}_0)]}\end{pmatrix}. \quad (16)$$

Applying inequality (15) to the transformed metric of Eq. (16), we find that $2\sqrt{\det[g^\alpha(\mathbf{k}_0)]} \geqslant |B_\alpha(\mathbf{k}_0)|$. Since $\mathbf{k}_0$ is arbitrary, we conclude that

$$\det[g^\alpha(\mathbf{k})] \geqslant \frac{|B_\alpha(\mathbf{k})|^2}{4} \quad (17)$$

for any $\mathbf{k}$ in the BZ. Furthermore, since

$$\int_{BZ} dk_x dk_y\,[B_\alpha(\mathbf{k})]^2 \geqslant A_{BZ}\bar{B}^2_\alpha, \quad (18)$$

it follows that

$$\int_{BZ} dk_x dk_y\,\det[g^\alpha(\mathbf{k})] \geqslant \frac{A_{BZ}\bar{B}^2_\alpha}{4} = \frac{\pi^2 C^2_\alpha}{A_{BZ}}. \quad (19)$$

Thus the integral of the determinant of the FS metric is bounded from below by a number which is proportional to the square of the topological invariant of the band.

Consider now the case when inequality (19) is saturated and the FS metric is uniform in the BZ. Inequality (19) is saturated when $\det[g^\alpha(\mathbf{k})] = \frac{|B_\alpha(\mathbf{k})|^2}{4}$ at all points $\mathbf{k}$ in the BZ and when, in addition, the Berry curvature is uniform in the BZ. From the constancy of the FS metric and the saturation

of inequality (17), it follows that there is some matrix t' such that

$$t' g^{\alpha}(\mathbf{k})(t')^{T} = \begin{pmatrix} \frac{\bar{B}_{\alpha}}{2} & 0 \\ 0 & \frac{\bar{B}_{\alpha}}{2} \end{pmatrix}, \tag{20}$$

where we have assumed without loss of generality that $\bar{B}_{\alpha} > 0$. If x', y' are the corresponding transformed position operators, from Eq. (10) and the above conditions, it follows that

$$\sum_{\mathbf{k},\gamma} \langle \mathbf{k},\gamma | P_{\alpha}(x'+iy') Q_{\alpha}(x'-iy') P_{\alpha} | \mathbf{k},\gamma \rangle = 0. \tag{21}$$

This implies that the trace of $DD^{\dagger} = 0$, where $D = Q_{\alpha}(x'-iy')P_{\alpha}$. Since $DD^{\dagger}$ is a positive-definite matrix, we may conclude that $Q_{\alpha}(x'-iy')P_{\alpha} = 0$. Let $q'_a = \sum_b t'^{-1}_{ba} q_b$. Writing the density operator $\rho_{\mathbf{q}}$ as $e^{-i\mathbf{q}\cdot\mathbf{r}} = e^{-i\mathbf{q}'\cdot\mathbf{r}'} = e^{-\frac{i}{2}\{(q'_x+iq'_y)(x'-iy')+(q'_x-iq'_y)(x'+iy')\}}$, it is easy to verify that the density operators satisfy a generalized metric-dependent version of the W_{∞} algebra:

$$[\bar{\rho}_{\mathbf{q}_1}, \bar{\rho}_{\mathbf{q}_2}] = 2i \sin\left(\frac{\mathbf{q}_1 \wedge \mathbf{q}_2 \bar{B}_{\alpha}}{2}\right) e^{q_{1l} g^{\alpha}_{lm} q_{2m}} \bar{\rho}_{\mathbf{q}_1+\mathbf{q}_2}. \tag{22}$$

The effective Hamiltonian projected to the Chern band can then also be written as

$$H_{\mathrm{LLL}} = \frac{1}{2} \int \frac{d^2\mathbf{q}}{(2\pi)^2} v(\mathbf{q})(\overline{\rho}_{\mathbf{q}} \overline{\rho}_{-\mathbf{q}} - \rho_{\mathbf{0}} e^{-q_l g^{\alpha}_{lm} q_m}), \tag{23}$$

where $\overline{\rho}_{\mathbf{q}}$ here is now the projected many-body density operator. This Hamiltonian has the same form as the effective Hamiltonian of the LLL [14] including the form factor in the second term.

IV. DISCUSSION

In summary, if $\int_{BZ} dk_x dk_y \det[g^{\alpha}(\mathbf{k})] = \frac{\pi^2 C_{\alpha}^2}{A_{BZ}}$ and if the Fubini-Study metric is uniform in the BZ, the density operators satisfy a closed algebra which is a generalization of the usual W_{∞} algebra. We note several interesting features. First, the Berry curvature and the FS metric both appear in this form of the W_{∞} algebra. Thus the algebra also applies to bands which have a higher Chern number and which therefore differ fundamentally from Landau levels which have a Chern number of 1. Second, we observe that the conditions under which we get a closed algebra of the projected density operators can be stated purely in terms of the FS metric.

For a system where the ideal conditions under which this algebra is obtained do not hold, the degree of deviation from these conditions provides a new parameter (or a set of parameters, depending on how one chooses to quantify the deviation) to predict how favorable a Chern band is for hosting FQHE-like physics. Subsequent numerical studies have confirmed this picture for a number of models [34]. Conversely, if one finds fractional topological phases in systems where the deviations from these conditions is considerable, one could argue that the physics of those systems is new and different from the conventional fractional quantum Hall effect.

The effects of disorder also enter the Hamiltonian through terms that involve the projected density operator. This suggests that the effects of disorder in the Chern band are likely to be the same as in the LLL when the conditions stated above for the FS metric are satisfied.

Let us briefly discuss other band structures where fractional phases may arise [35–37]. One primary example is topological bands with time-reversal symmetry. Consider, for instance, the case of Z_2 insulators with a pair of time-reversed paired flat bands. The band projection operator P can then always be written as a sum $P = P_1 + P_2$, where P_1 and P_2 are a pair of projectors related by time-reversal symmetry, which have Chern numbers associated with them that are equal in magnitude and opposite in sign [38,39]. There may be circumstances where the interactions between electrons with different indices can be neglected either due to the nature of the physical interactions or due to the formation of fractionalized states where the role of such interactions are minimized. Then the relevant projected density operators are $P_i \rho_{\mathbf{q}} P_i$ $(i = 1,2)$, and the conditions under which these form a closed algebra are the uniformity of the FS metric associated with each projection operator and the saturation of inequality (19) for the same.

The current work highlights the important role of quantum geometric features of bands in fractional topological insulators. An illustration of the quantum band geometry of a lattice model is provided in the Appendix. The key implication of this and related work [13] is that a fractional topological insulator phase does not derive topological stability from the Chern invariant alone; rather, its stability depends on the details of the geometry of the Hilbert space of the single-particle Bloch basis states. The deformations of the quantum geometry needed to stabilize or destabilize a topological phase can be identified through the Fubini-Study metric and the Berry curvature. Given this dependence on the geometry of these states, one is tempted to even go so far as to suggest that the

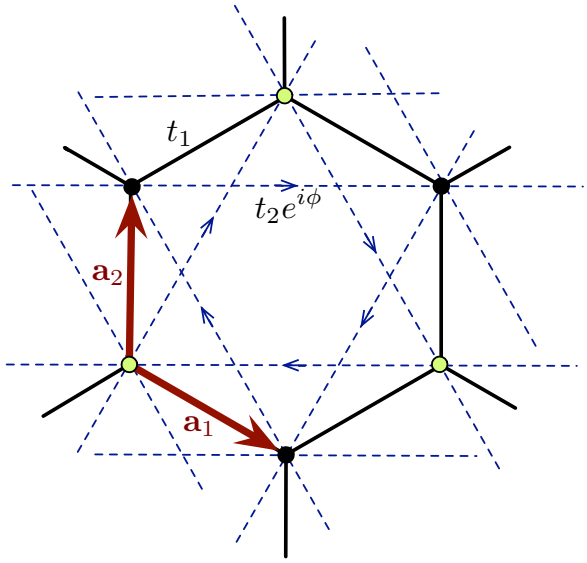

FIG. 1. (Color online) The hexagonal unit cell for a tight-binding model on the honeycomb lattice with nontrivial Chern insulator phases. t_1 and $t_2 e^{i\pm\phi}$ are the nearest- and next-nearest-neighbor hopping amplitudes. The model also includes a term that gives on-site energies of M and $-M$ to the two triangular sublattices.

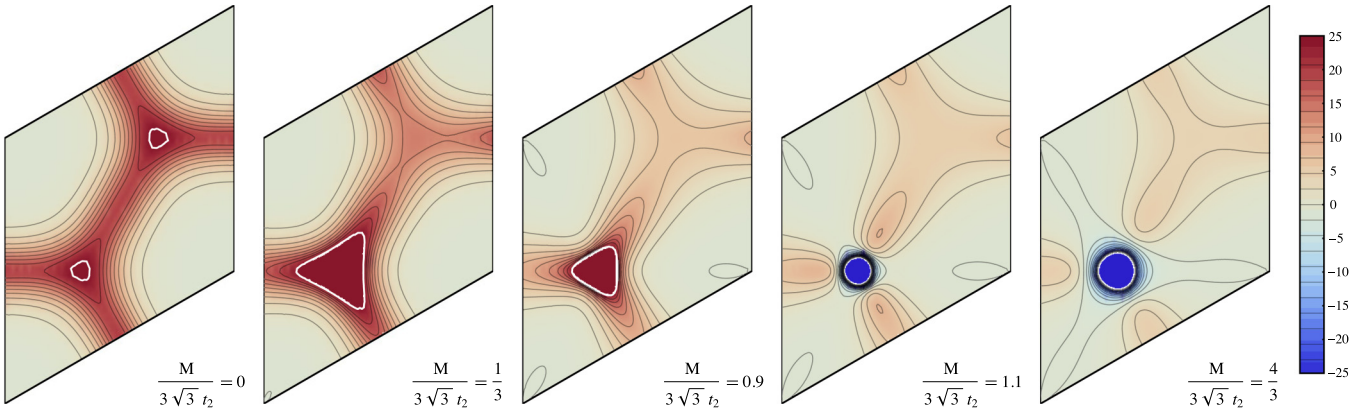

FIG. 2. (Color online) Contour plots of the distribution of Berry curvature over a unit cell of the reciprocal lattice; this unit cell was chosen so as to not split up the Brillouin-zone corners, which appear to be points of high Berry curvature. The same color scale is used in each panel.

term "fractional topological insulators" should be replaced by "fractional geometric insulators."

ACKNOWLEDGMENTS

I thank T. S. Jackson for useful discussions and continuing collaboration and for allowing me to use some of the figures he has generated, and S. Paramewsaran and S. L. Sondhi for discussions, comments, and an earlier collaboration. Additionally, I would like to thank S. Chakarvarty, J. T. Chalker, S. H. Simon and R. Shankar for helpful conversations and comments.

APPENDIX: QUANTUM BAND GEOMETRY OF THE HALDANE MODEL

In this section, we describe the quantum band geometry of the Haldane model. This model has a tight-binding Hamiltonian with a matrix function $h(\mathbf{k})$:

$$h(\mathbf{k}) = n_0(\mathbf{k}) + \sum_{i=1}^{3} n_i(\mathbf{k})\sigma_i = n_0 + \mathbf{n}\cdot\boldsymbol{\sigma}, \tag{A1}$$

where

$$n_0 = 2t_2\cos\phi\sum_i \cos\mathbf{k}\cdot\mathbf{b}_i, \tag{A2}$$

$$n_1 = t_1\sum_i \cos\mathbf{k}\cdot\mathbf{a}_i, \tag{A3}$$

$$n_2 = t_1\sum_i \sin\mathbf{k}\cdot\mathbf{a}_i, \tag{A4}$$

$$n_3 = M - 2t_2\sin\phi\sum_i \sin\mathbf{k}\cdot\mathbf{b}_i. \tag{A5}$$

Here, the vectors $\mathbf{a}_i, \mathbf{b}_i$ are the nearest- and next-nearest-neighbor displacements on the honeycomb lattice, σ_i are the usual Pauli sigma matrices, t_1 is the nearest-neighbor (intersublattice) hopping amplitude, $t_2 e^{\pm i\phi}$ are the chiral next-nearest-neighbor hopping amplitudes, and M is an inversion symmetry-breaking term that gives on-site energies of M and $-M$ to sites on the two triangular sublattices of the honeycomb lattice (Fig. 1). We obtain a Chern band (with Chern number $C = \pm 1$) for

$$\left|\frac{M}{t_2}\right| < 3\sqrt{3}|\sin\phi|. \tag{A6}$$

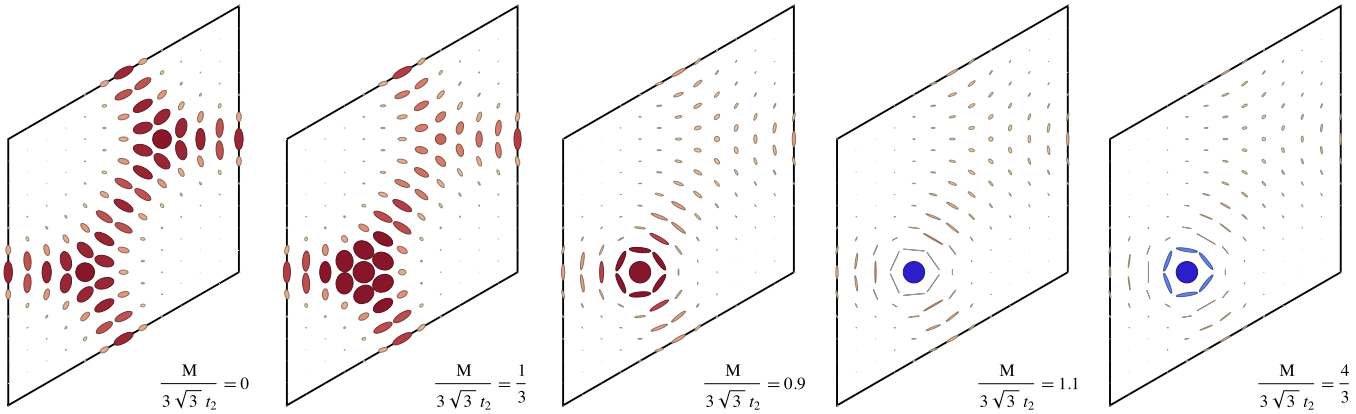

FIG. 3. (Color online) Characteristic ellipsoids corresponding to the quantum metric, i.e., the region satisfied by $\mathbf{x}\cdot g\cdot\mathbf{x} < 1$. Colors are taken from the Berry curvature.

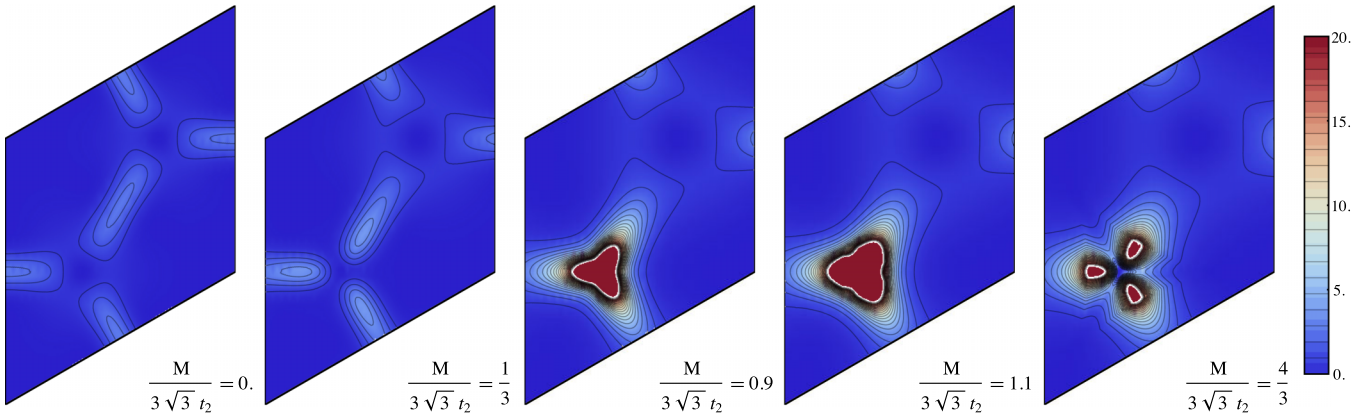

FIG. 4. (Color online) Contour plots of $\mathrm{tr}[g] - |B|$, i.e., the difference between the trace of the quantum metric and the absolute value of the Berry curvature, for the same parameter values.

This model is of interest to us because a number of studies [8–12] have provided evidence that with an appropriate density-density interaction and flattening of the band, topological phases are formed in this model at certain fractional fillings, which provides an avenue for testing some of our conclusions. We draw some plots illustrating the quantum geometry of this model for a set of different parameters below and show how the quantum geometry can be used to predict which parameter choice would be the most favorable for fractionalized topological phases. All of the following plots are made at the parameter values $t_2/t_1 = 1/6$ and $\phi = \pi/2$; we then plot quantities of interest for values of M in both the $C = 1$ and $C = 0$ phases. The first three plots in Figs. 2, 3, and 4 correspond to the nontrivial Chern phase, and the last two correspond to the trivial phase.

In Fig. 2, we plot the Berry curvature of the lower band in a unit cell of the reciprocal lattice. We notice that the Berry curvature is most uniform in the first plot and gets more and more concentrated at one of the Brillouin-zone corners as the value of $\frac{M}{3\sqrt{3}t_2}$ gets closer to 1. At $\frac{M}{3\sqrt{3}t_2} = 1$, there is a Dirac point at the Brillouin-zone corner, and some remnants of this are visible in the form of peaked Berry curvature even in the trivial phase, as can be seen in the last two plots.

In Fig. 3, we have plotted the characteristic ellipsoids corresponding to the quantum metric for the lower band, i.e., the region satisfied by $\mathbf{x} \cdot g \cdot \mathbf{x} < 1$, at several points in the unit cell of the reciprocal lattice. The sizes of these ellipsoids are proportional to the determinant of the metric at the given point in momentum space, and the shape gives us an idea of the relative magnitude of the different components of the quantum metric. The arguments presented in the main text lead us to conclude that the conditions most favorable for fractionalized phases correspond to a uniform metric whose characteristic ellipsoid is a circle of the same size everywhere in the Brillouin zone. We see that the leftmost plot in Fig. 3 again has the most uniform characteristic ellipsoids and is thus closest to the ideal conditions.

In Fig. 4, we have plotted $\mathrm{tr}[g] - |B|$ for the lower band. From Eq. (15), we know that this quantity is always nonnegative and that the most favorable conditions correspond to this quantity being uniformly zero in the Brillouin zone. The plot for $\frac{M}{3\sqrt{3}t_2} = 0$ looks quite similar to that for $\frac{M}{3\sqrt{3}t_2} = \frac{1}{3}$ but far closer to the ideal conditions than the plot for $\frac{M}{3\sqrt{3}t_2} = 0.9$.

Thus, based on these plots, we expect that the Haldane model for $\frac{M}{3\sqrt{3}t_2} = 0$ would be more suitable for hosting fractionalized topological phases than the other points. This prediction is borne out by doing exact diagonalization studies for small systems (with eight particles), which shows that the gap for a $\nu = 1/3$ FQHE state among the various points studied here is highest for $\frac{M}{3\sqrt{3}t_2} = 0$. Related work [34] also suggests that similar trends hold for some other models such as the kagome lattice model of Ref. [25].

[1] M. Z. Hasan and C. L. Kane, Rev. Mod. Phys. **82**, 3045 (2010).
[2] X. L. Qi and S. C. Zhang, Rev. Mod. Phys. **83**, 1057 (2011).
[3] M. Hasan and J. Moore, Annu. Rev. Condens. Matt. Phys. **2**, 55 (2011).
[4] K. v. Klitzing, G. Dorda, and M. Pepper, Phys. Rev. Lett. **45**, 494 (1980).
[5] D. J. Thouless, M. Kohmoto, M. P. Nightingale, and M. den Nijs, Phys. Rev. Lett. **49**, 405 (1982).
[6] F. D. M. Haldane, Phys. Rev. Lett. **61**, 2015 (1988).
[7] H. L. Stormer, A. Chang, D. C. Tsui, J. C. M. Hwang, A. C. Gossard, and W. Wiegmann, Phys. Rev. Lett. **50**, 1953 (1983).
[8] T. Neupert, L. Santos, C. Chamon, and C. Mudry, Phys. Rev. Lett. **106**, 236804 (2011).
[9] D. Sheng, Z. Gu, K. Sun, and L. Sheng, Nat. Commun. **2**, 389 (2011).
[10] N. Regnault and B. A. Bernevig, Phys. Rev. X **1**, 021014 (2011).
[11] T. Scaffidi and G. Möller, Phys. Rev. Lett. **109**, 246805 (2012).
[12] A. M. Läuchli, Z. Liu, E. J. Bergholtz, and R. Moessner, Phys. Rev. Lett. **111**, 126802 (2013).
[13] S. A. Parameswaran, R. Roy, and S. L. Sondhi, Phys. Rev. B **85**, 241308 (2012).
[14] S. M. Girvin, A. H. MacDonald, and P. M. Platzman, Phys. Rev. B **33**, 2481 (1986).

[15] S. M. Girvin, A. H. MacDonald, and P. M. Platzman, Phys. Rev. Lett. **54**, 581 (1985).
[16] A. Cappelli, C. Trugenberger, and G. Zemba, Nucl. Phys. B **396**, 465 (1993).
[17] D. Karabali, Nucl. Phys. B **428**, 531 (1994).
[18] X. L. Qi, Phys. Rev. Lett. **107**, 126803 (2011).
[19] J. McGreevy, B. Swingle, and K.-A. Tran, Phys. Rev. B **85**, 125105 (2012).
[20] Y. M. Lu and Y. Ran, Phys. Rev. B **85**, 165134 (2012).
[21] R. B. Laughlin, Phys. Rev. Lett. **50**, 1395 (1983).
[22] G. Murthy and R. Shankar, arXiv:1108.5501.
[23] G. Murthy and R. Shankar, Phys. Rev. B **86**, 195146 (2012).
[24] M. O. Goerbig, Eur. Phys. J. B **85**, 15 (2012).
[25] E. Tang, J.-W. Mei, and X.-G. Wen, Phys. Rev. Lett. **106**, 236802 (2011).
[26] K. Sun, Z. Gu, H. Katsura, and S. Das Sarma, Phys. Rev. Lett. **106**, 236803 (2011).
[27] I. I. Kogan, Int. J. Mod. Phys. A **09**, 3887 (1994).
[28] The effective Hamiltonian for the LLL written in terms of the many-body density operators also has a form factor not present in Eq. (4). We will show later that this form factor has an exact analog in the Chern insulator problem provided the algebras are the same.
[29] Y. L. Wu, B. A. Bernevig, and N. Regnault, Phys. Rev. B **85**, 075116 (2012).
[30] D. N. Page, Phys. Rev. A **36**, 3479 (1987).
[31] J. Anandan and Y. Aharonov, Phys. Rev. Lett. **65**, 1697 (1990).
[32] S. Kobayashi and K. Nomizu, *Foundations of Differential Geometry* (Interscience, New York, 1969), Vol. 2.
[33] A. K. Pati, Phys. Lett. A **159**, 105 (1991).
[34] T. S. Jackson, G. Möller, and R. Roy, arXiv:1408.0843.
[35] M. Levin and A. Stern, Phys. Rev. Lett. **103**, 196803 (2009).
[36] M. Levin, F. J. Burnell, M. Koch-Janusz, and A. Stern, Phys. Rev. B **84**, 235145 (2011).
[37] T. Neupert, L. Santos, S. Ryu, C. Chamon, and C. Mudry, Phys. Rev. B **84**, 165107 (2011).
[38] R. Roy, Phys. Rev. B **79**, 195321 (2009).
[39] R. Roy, New J. Phys. **12**, 065009 (2010).